Influence of anisotropy of Compton scattering on low energy x-ray reflection

2004 J. Phys. D: Appl. Phys. 37 2314

(http://iopscience.iop.org/0022-3727/37/16/014)

INSTITUTE OF PHYSICS PUBLISHING JOURNAL OF PHYSICS D: APPLIED PHYSICS

J. Phys. D: Appl. Phys. **37** (2004) 2314–2317 PII: S0022-3727(04)79014-2

Influence of anisotropy of Compton scattering on low energy x-ray reflection

D M Davidović[1,3], J Vukanić[1] and D Arsenović[2]

[1] The Vinča Institute of Nuclear Sciences, PO Box 522, Belgrade, Serbia
[2] Institute of Physics, Pregrevica 118, PO Box 57, Belgrade, Serbia

E-mail: davidd@vin.bg.ac.yu, vukanic@vin.bg.ac.yu and arsenovic@phy.bg.ac.yu

Received 13 April 2004
Published 28 July 2004
Online at stacks.iop.org/JPhysD/37/2314
doi:10.1088/0022-3727/37/16/014

Abstract
The reflection of x-rays from a semi-infinite water target, for energies ranging from 10 to 60 keV, often used in x-ray diagnostics, is investigated by Monte Carlo simulation. The same process was also treated analytically as the classical albedo problem for isotropic scattering without energy loss. Good agreement of results for the angular distribution of reflected photons of the two approaches is obtained for higher photon energies from the energy range considered. Multiple collision scattering dominates at higher energies, leading to isotropization of the photon distribution. Discrepancies between the isotropic scattering model and Monte Carlo results appear at the lower part of the energy range. Monte Carlo results show that at these energies photon reflection is governed mainly by single collisions and that these discrepancies are caused by anisotropy of the distribution of single backscattered photons. It is shown that the inclusion of the anisotropy of single Compton backscattering in the analytical model greatly improves the agreement with Monte Carlo results.

1. Introduction

Under certain idealizations and simplifications it is possible to derive theoretically important relations that describe the behaviour of photons reflected from a half space. Within a model that assumes multiple isotropic scattering of photons without energy loss the angular distribution of backscattered photons is given by an exact solution [1, 2],

$$R(\mu_0, \mu) = \frac{\omega}{2}\frac{\mu}{\mu + \mu_0} H(\omega, \mu_0) H(\omega, \mu). \tag{1}$$

Here, μ_0 and μ are the directional cosines of the incident and reflected photons with respect to the target surface normal. $H(\omega, \mu)$ is the H function that is tabulated for various values of the variable μ and the parameter ω [1, 3]. The scattering medium is characterized only through the parameter ω, which is given by

$$\omega = \frac{\sigma_R}{\sigma_R + \sigma_a}, \tag{2}$$

where σ_R is the total cross section for Compton scattering and σ_a is the total cross section for photoabsorption. Both cross sections are calculated per atom.

For large ω ($\omega \approx 1$), the reflection is dominated by photons that have scattered so many times that the correlation with the original preferred direction is lost, so that the distribution of photons becomes isotropic in character, and due to this the main assumptions of the model are realistic in this case. In the opposite situation, when ω is small ($\omega \ll 1$), the reflection is essentially determined by single backscattering events and depends now on the details of the differential cross section that are not included in the above model. These model considerations are confirmed by the results of Monte Carlo simulation for x-ray reflection from water given in table 1 below. We present the total number of reflected photons as a function of photon incident energy, classified according to the number, n, of collisions suffered ($n = 1, 2, 3, 4$ and $n > 4$). The history of 100 000 photons incident normally on a water target was followed.

Looking at table 1, one can see that at lower energies the single collision reflection is absolutely dominant. With

[3] Author to whom any correspondence should be addressed.

Table 1. Reflection of photons from water for different energies, obtained by Monte Carlo simulation. The total number of photons considered was 100 000, n represents the number of collisions before reflection and n_a is the number of absorbed photons.

E [keV]	10	15	20	30	40	50	60
$n = 1$	1 321	3 049	5 504	10 007	12 221	13 283	13 692
$n = 2$	57	367	1 055	3 836	5 954	7 285	8 076
$n = 3$	4	51	287	1 590	3 476	4 672	5 494
$n = 4$	0	8	79	744	2 134	3 184	3 970
$n > 4$	0	2	29	860	4 451	10 435	16 925
n_a	98 618	96 523	93 046	82 963	71 764	61 141	51 843

increasing energy, the number of photons reflected in multiple scattering events increases, so that at energies near 60 keV, this kind of reflection dominates. Because of this, it is of interest to develop an analytic model that deals with these two extreme situations. The development of such a model which takes into account the scattering anisotropy, in particular at low energies, will be given in the next section.

2. Analytical model for reflection of photons from a half space

A scheme of the single collision backscattering event is shown in figure 1. A photon with energy E_0 is incident at an angle α_0 ($\cos\alpha_0 = \mu_0$) with respect to the target surface normal and penetrates the target. The probability for the initial photon passing the distance l along the straight line without any interaction is taken into account by the exponential factor $\exp(-n\sigma_T l)$, where σ_T is the total cross section for attenuation of the beam per atom, $\sigma_T = \sigma_R + \sigma_a$, and n is the number of atoms per unit volume. In a Compton collision with an electron of the target atom, which occurs at path length x/μ_0, where x is the inward coordinate normal to the surface, the photon is scattered through the angle θ, and after travelling the path length x/μ, it leaves the target. Here, $\mu = \cos\alpha$, and α and φ are the polar and azimuthal angles of the photon exit direction with respect to the target surface normal. The scattering angle, θ, is related to the directional cosines, μ_0 and μ, and azimuth, φ, by

$$\cos\theta = -\mu_0\mu + \sqrt{1-\mu_0^2}\sqrt{1-\mu^2}\cos\varphi. \tag{3}$$

Within the single collision model, the total probability, $R_S(\mu_0, \mu, \varphi)\mathrm{d}\mu\,\mathrm{d}\varphi$, for the observed photon to be backscattered into the solid angle $\mathrm{d}\mu\,\mathrm{d}\varphi$, including all penetration depths x through an infinitely thick target, is given by

$$R_S(\mu_0, \mu, \varphi)\mathrm{d}\mu\,\mathrm{d}\varphi = n\frac{\mathrm{d}\sigma(\theta)}{\mathrm{d}\Omega}\mathrm{d}\mu\,\mathrm{d}\varphi \times \int_0^\infty \mathrm{e}^{-n\sigma_T x((1/\mu_0)+(1/\mu))}\frac{\mathrm{d}x}{\mu_0}. \tag{4}$$

Here $\mathrm{d}\sigma(\theta)/\mathrm{d}\Omega$ is the differential cross section for photon scattering calculated per atom, and $\mathrm{d}\Omega$ is the elementary solid angle.

The probability, $R_S(\mu_0, \mu)\,\mathrm{d}\mu$, for a photon to be reflected with directional cosines between μ and $\mu + \mathrm{d}\mu$, irrespective of the azimuth, follows by integration of equation (4) over all azimuthal angles. Performing integration over x in

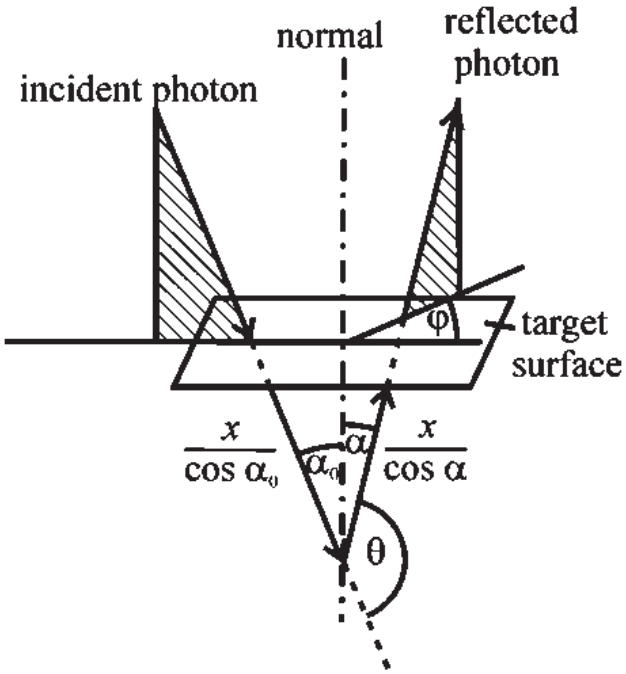

Figure 1. Geometry of the single backscattering event.

equation (4), the quantity $R_S(\mu_0, \mu)$ may be represented in the form

$$R_S(\mu_0, \mu) = \int_0^{2\pi} R(\mu_0, \mu, \varphi)\mathrm{d}\varphi = \frac{\mu}{\mu_0 + \mu}\frac{1}{\sigma_T}\int_0^{2\pi}\frac{\mathrm{d}\sigma(\theta)}{\mathrm{d}\Omega}\,\mathrm{d}\varphi. \tag{5}$$

Assuming that the scattering is isotropic, one has

$$\frac{\mathrm{d}\sigma}{\mathrm{d}\Omega} = \frac{\sigma_R}{4\pi}, \tag{6}$$

where σ_R is the total Compton scattering cross section. Inserting equation (6) into equation (5), one obtains the isotropic distribution of photons backscattered in single collisions,

$$R_S(\mu_0, \mu) = \frac{1}{2}\frac{\mu}{\mu_0 + \mu}\omega. \tag{7}$$

The same result follows from equation (1) in the single collision region: for small values of the parameter $\omega(\omega \ll 1)$, for any value of the variable μ, $H(\omega, \mu) \approx 1$ and equations (1) and (7) become identical. For the single collision region $\omega \ll 1$, instead of using the isotropic approximation from equation (6), one can include the differential cross section given by the

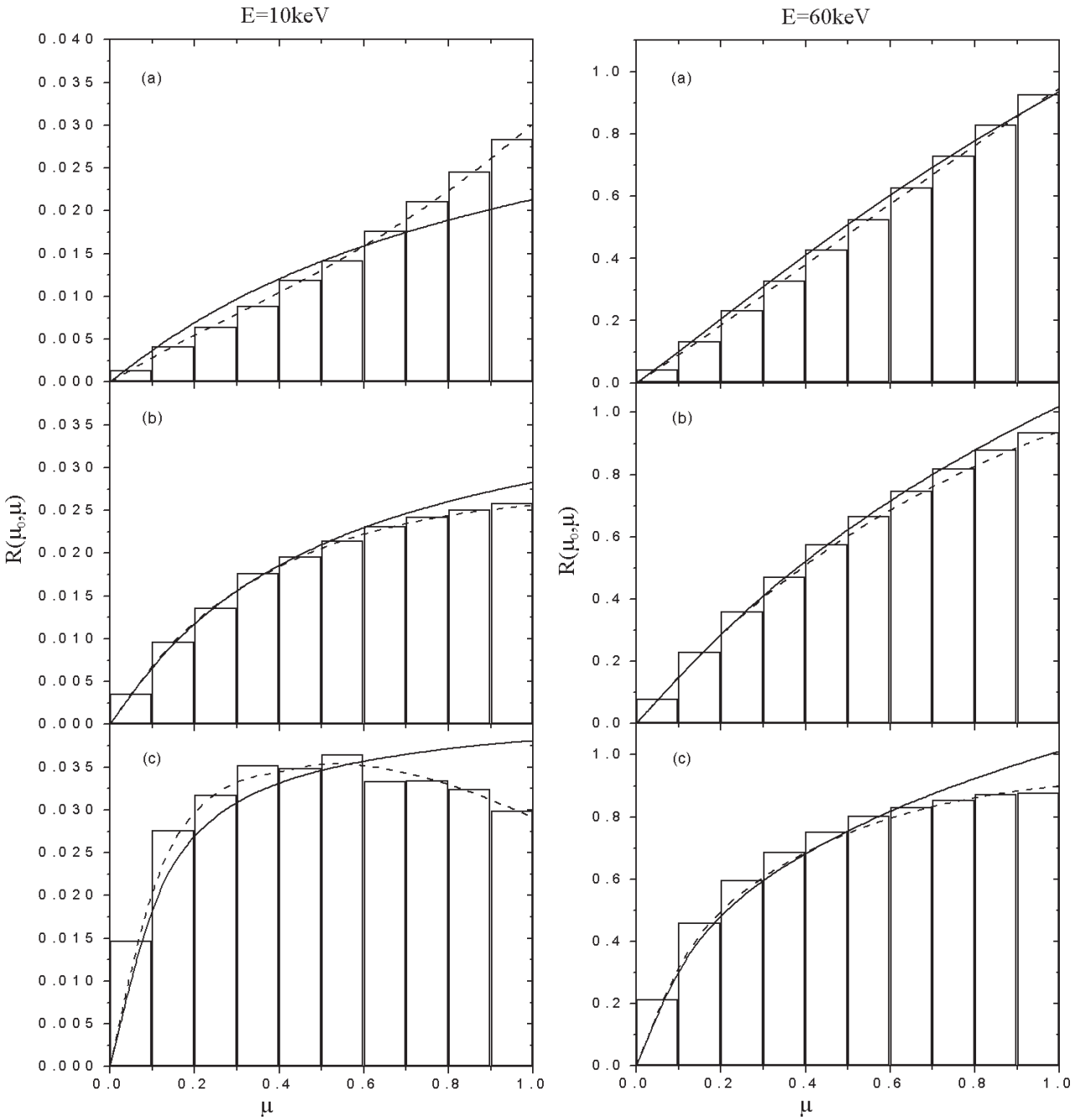

Figure 2. Angular distribution of backscattered photons for photon energies $E = 10$ keV (left panel) and $E = 60$ keV (right panel), calculated for normal incidence ($\mu_0 = 1$) (*a*), oblique incidence ($\mu_0 = 0.5$) (*b*) and grazing incidence ($\mu_0 = 0.1$) (*c*). ——, results from isotropic model (equation (1));. . . . . , results according to equation (10), which includes single backscattering anisotropy. Histograms are from Monte Carlo simulations.

Klein Nishina formula [4], which at low energies gets a simpler form:

$$\frac{\mathrm{d}\sigma(\theta)}{\mathrm{d}\Omega} = \frac{3}{16\pi}\sigma_{\mathrm{R}}(1+\cos^2\theta)\left(1+\frac{2\gamma}{1-2\gamma}\cos\theta\right), \qquad (8)$$

where γ is the ratio of the photon incident energy to the electron rest energy. By inserting equation (8) for the differential cross section into equation (5) after integration, one obtains a more accurate expression for the angular distribution of reflected photons in the single collision approximation

$$R_{\mathrm{S}}^{\mathrm{a}}(\mu_0,\mu) = \frac{\omega}{16}\frac{\mu}{\mu_0+\mu}\left\{(1-3\mu_0^2)(1-3\mu^2)+8 - \frac{3}{5}\left(\frac{2\gamma}{1-2\gamma}\right)\mu_0\mu[(3-5\mu_0^2)(3-5\mu^2)+16]\right\}. \qquad (9)$$

This is an improved result compared with equation (7) because here the assumption of isotropic scattering is removed.

The model exact isotropic distribution given by equation (1) may be developed in a series in powers of ω, where the term containing the factor ω^n represents the contribution of

photons reflected through n collisions. In this model, all these collisions are described by the isotropic cross section given by equation (6). The first term of this series, which is linear in ω, is given by equation (7). Replacing this term with the accurate expression given by equation (9), in which the anisotropy of Compton scattering is taken into account, we obtain

$$R^{\mathrm{a}}(\mu_0, \mu) = \frac{\omega}{2}\frac{\mu}{\mu_0 + \mu} H(\omega, \mu_0) H(\omega, \mu) + [R^{\mathrm{a}}_{\mathrm{S}}(\mu_0, \mu) - R_{\mathrm{S}}(\mu_0, \mu)]. \quad (10)$$

Formula (10) covers the whole range of ω. For small ω it tends to the formula (9), while for the high ω it does not differ much from formula (1). Formula (10) represents our main theoretical result. It improves the isotropic model by inclusion of anisotropy of Compton scattering in single backscattered events. The importance of this refinement will be seen in the next section.

3. Results and discussion

The most characteristic results of all the above described approaches are given in figure 2. The model results obtained from equations (1) and (10) are compared with the results of Monte Carlo simulation for water as a scatterer. We have chosen two extreme points of our energy interval, 10 and 60 keV, and give the results for different photon incidence.

For 10 keV incident photon energy, the parameter ω is very small ($\omega = 0.0806$), and reflection is essentially determined by single backscattering events, and in this case it depends on the details of the differential cross section because of the lack of multiple scattering isotropization. This explains the discrepancies between the isotropic distribution calculated from equation (1) (the full lines) and the Monte Carlo histograms visible in the left panel of figure 2. The dashed lines, obtained from equation (10), greatly improve the agreement with the Monte Carlo results, both in the shape of the distribution and in the magnitude. Note that this equally holds for normal, oblique and grazing incidence. So, replacing the contribution of single scattering events described by an isotropic cross section with those described by a Klein Nishina cross section improves the results for the angular distribution for different angles of incidence. This agreement further substantiates the claim that single backscatter events are the predominant mode of scatter at lower energies.

In figure 2, on the right panel, the angular distribution of reflected photons is presented for the photon energy of 60 keV and different angles of photon incidence. At 60 keV photon energy, the parameter ω is large ($\omega = 0.936$). It is seen that, although the isotropic and anisotropic analytical results are close, the dashed curves tend to improve the agreement with the results of the Monte Carlo simulation for different photon incidence.

Altogether, our results show that for energies 10–60 keV, often used in x-ray diagnostics, the improved formula (10) gives good agreement with simulation data. Therefore, the simple anisotropic model developed in this work, may be considered as reliable and sufficiently accurate in this energy range, both for normal and oblique photon incidence.

Acknowledgments

The authors are grateful to the Ministry of Science and Environmental Protection of Republic of Serbia for financial support of this work.

References

[1] Chandrasekhar S 1960 *Radiative Transfer* (New York: Dover)
[2] Davidović D M, Vukanić J and Arsenović D 2003 *Phys. Med. Biol.* **48** N213
[3] Chilton A B, Shultis J K and Faw R E 1984 *Principles of Radiation Shielding* (Englewood Cliffs, NJ: Prentice Hall)
[4] Leipunovsky O I, Novozhilov V V and Sakharov V N 1960 *Gamma Ray Transport in Matter* (Moscow: Nauka) (in Russian)